

**Reply to comment by Witte *et al.* on
“Isochoric, isobaric, and ultrafast conductivities of
aluminum, lithium, and carbon in the warm dense matter regime”,
Phys. Rev. E **96**, 053206 (2017).**

M.W.C. Dharma-wardana* and D. D. Klug
National Research Council of Canada, Ottawa, Canada, K1A 0R6

L. Harbour and Laurent J. Lewis
Département de Physique, Université de Montréal, Montréal, Québec, Canada.
(Dated: May 9, 2019)

In Phys. Rev. E, **99**, 047201 (2019) Witte *et al.* have commented on our conductivity calculations [Phys. Rev. E **96**, 053206 (2017)] for warm dense matter (WDM). (i) They criticize our use of the spherically-averaged structure factor $S(k)$ for calculations of the static conductivity σ of FCC aluminum - a common approximation for polycrystalline materials. They themselves give no calculations as their method using density-functional theory (DFT) and molecular dynamics (MD) based Kubo-Greenwood (KG) calculations becomes impractical for cold ions. (ii) We are satisfied that Witte *et al.* no longer claim a factor of ~ 1.5 change in σ on changing the exchange-correlation (XC) functional used. (iii) They have provided computer-intensive calculations of σ for aluminum using DFT-MD-KG simulations, for temperatures T up to 15 eV but using only $N=64$ atoms in the simulation, where as a mixture of ionic species needs a far larger N to be credible. We present multi-species conductivity calculations via a parameter-free DFT theory [Phys. Rev. E. **52**, 5352 (1995)] for 5 eV to 50 eV. (iv) The conductivities obtained from well-converged DFT-MD-KG methods show a significant underestimate of σ ; this is especially evident for the isochoric conductivity σ_{ic} extrapolating to $\sim 3.5 \times 10^6$ S/m, i.e., *even below* the experimental *isobaric* value of 4.1×10^6 S/m at the melting point, when a value of $\sim 5 \times 10^6$ S/m is anticipated.

PACS numbers: 52.25.Os, 52.35.Fp, 52.50.Jm, 78.70.Ck

I. INTRODUCTION

Witte *et al.* [1] have commented on our work, Ref. [2], Ref. [3], referred to here as DW16 and DKHL respectively, while Witte *et al.* refer to both as DWD. Their comment is denoted here as “WitteC”. As DW16 involves only one author, this reply is confined to comments on DKHL, while DW16-issues will be addressed elsewhere. The static conductivities σ of Al, C and Li under warm dense matter (WDM) conditions were studied in DKHL using the *simplest implementation* of the neutral-pseudo-atom (NPA) model, as described in DKHL.

Our concern with Witte *et al.* arose from their Letter [4] where the isochoric conductivity σ_{ic} of aluminum at 2.7 g/cm^3 and temperature $T=0.3 \text{ eV}$ is calculated using the Kubo-Greenwood (KG) formula via density-functional theory (DFT) and molecular-dynamics (MD) simulations. The conductivity obtained with the semi-empirical Heyd-Scuseria-Ernzerhof (HSE) [5] exchange-correlation (XC) functional was 2.22×10^6 S/m (see Fig. 1, Ref. [4], and Fig. 1), while the Perdew-Burke-Ernzerhof (PBE) [6] functional gave 3.35×10^6 S/m. Such a large change (factor of ~ 1.5) on changing XC-functionals for a static property was surprising. The

claim of ‘better’ results in their Fig.1 using the HSE functional depended on just one experimental static conductivity from Gathers [7] Table-II, column 4., i.e., for $T = 0.3 \text{ eV}$, incorrectly taken to be for *isochoric* aluminum. In May 2017 this seemed a simple error in reading Gathers’ data and we suggested a minor correction.

In response, and as justification, Witte *et al.* sent their Li- σ comparisons with experimental data [11, 12]. Our NPA results on Li agree with theirs, except at $\rho = 0.6 \text{ g/cm}^3$ and $T = 4.5 \text{ eV}$ [13]. We also drew attention to the last row of Table 23 of Gathers’ 1986 review article [14] where the conductivities were clearly for the *isobaric* densities of aluminum.

We are satisfied that Witte *et al.* have modified their value for σ_{ic} using the HSE functional, differing from the σ_{ic} from PBE by $< 20\%$ (Fig. 1). Furthermore, in Ref. 10 they say: “Note that the conductivity values reported here at $T= 0.3 \text{ eV}$ for the HSE functional are slightly higher than those published earlier in Ref. 10, where a part of the non-local contributions in the transition matrix elements was not taken into account”. In Ref. 4 the conductivity σ_{ic} at 0.3 eV is given as 2.22×10^6 S/m, for 2.7 g/cm^3 while their corrected values are 2.82×10^6 S/m, while the value, i.e., σ_{ib} at 1.87 g/cm^3 is 1.62×10^6 S/m.

They now treat the Gathers’ experimental results as being isobaric, thus correcting our main concern. The difference between column 4 and column 5 of Gathers is of the order of 10-25% as seen in Fig. 2, or from Table I

* Email address: chandre.dharma-wardana@nrc-cnrc.gc.ca

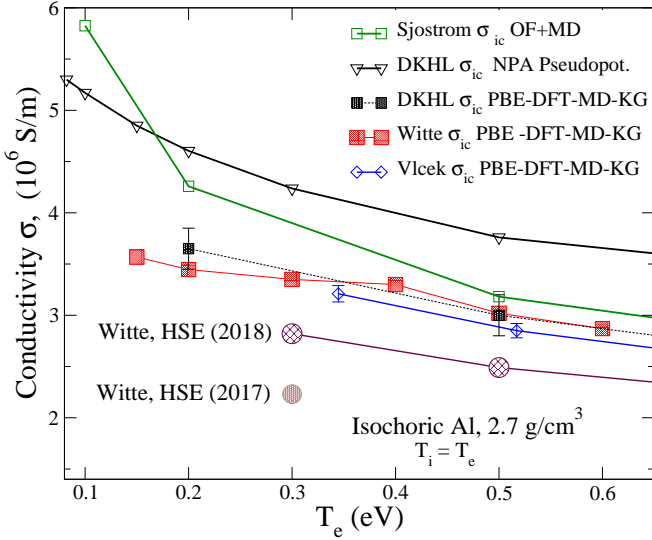


FIG. 1. (Color online) Isochoric conductivities σ_{ic} of aluminum from near its melting point to about 0.6 eV; our DFT+MD data and those of Vlček [8], Sjöström *et al.* [9] are shown. The Witte *et al.* [4] calculation of σ_{ic} at $T = 0.3$ eV and $\rho = 2.7$ g/cm³ using the PBE and HSE functionals in 2017, and in 2018, are also shown.

of Ref. [3]. Gathers does not measure the temperature, but estimates it from the heat input. As seen in the discussion in Gathers (even in regard to his experiments on copper), the raw resistivities, measured as a function of the input enthalpy H has to be corrected for volume expansion to determine the temperature associated with that input enthalpy. This correction is included in Gathers' column 5.

II. DETAILED CONSIDERATIONS

We discuss the issues raised in WitteC in more detail below.

A. Use of the Ziman formula — Comment item (i)

The WitteC criticizes the spherically-averaged $S(k)$ approximation proposed in Sec. II-C of DKHL. The spherical average was used in calculating ultra-fast conductivities σ_{uf} for two-temperature ($2T$) experiments on polycrystalline samples of cubic crystals [15]. The spherical average applies to polycrystalline materials when the probe beam samples a large enough volume.

There was no mention of the use of a single crystal in the LCLS experiment. In fact, a 50 μm thick aluminum foil and a beam of up to 10 μm had been used. If Neumeyer's data (cited as a private communication in the comment by Witte *et al.*) was for the same foil and averaging over the same volume as the LCLS beam, then the report on the experiment given in Ref. [15] needs

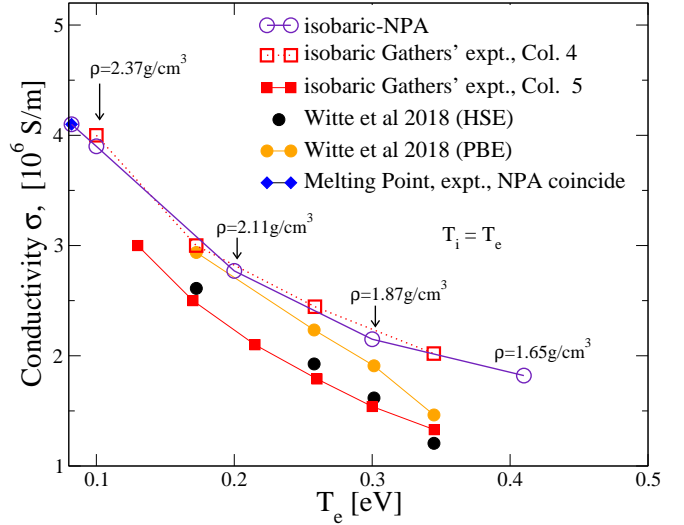


FIG. 2. (Color online) The isobaric conductivities σ_{ib} of aluminum from its melting point to about 0.4 eV. Here we use Fig. 9 of Witte *et al.* revised calculations [10], Gathers' experimental data, and our NPA-Ziman calculations [3]. We claim that the valid experimental data set is Gathers' Column 4 (empty red squares) which aligns correctly with the value at the melting point, while Witte *et al.* claim that the correct experimental data set is Gathers' Column 5 (filled red squares). In Ref. [4] Witte claimed that Gathers' column 4 data were isochoric conductivities, provoking our disagreement.

a correction. When the papers DW16 and DKHL were written, Ref. [15] was the only published source of information on the experiment and there the aluminum was claimed to be a plasma with $T_i = T_e = 6\text{eV}$. Their claim that $T_i = 6$ eV was not credible, and we explored a $2T$ model with cold ions but there was no reason to use a crystal-like model. In Witte's comment they now claim that the $S(k)$ has the crystalline features of a cold-ion subsystem. Thus the analysis by Sperling *et al.* [15] needs an erratum to ensure that other readers will be aware of the nature of the sample used.

An averages $S(k)$ arises naturally with polycrystalline samples. The laser beam averages over a volume of 10 μm diameter and depth of 50 μm . The Laue peaks broaden and fill the k -regions, as in the spherical average. The possibility of improving the theory and experiment using single crystals was already stated by us in DKHL thus:

"Hence this calculation appears to need further improvement for $T < 1.0$ eV, e.g., using the structure factor of the FCC solid and ... band-structure effects".

So WitteC's concern is already voiced by us. No crystalline $S(k)$ was reported in Ref. [15] which claimed that the ions were at 6 eV. Our papers were based on the available information.

Furthermore Witte *et al.* seem to suggest that the NPA method cannot generate the needed solid-state structure factor for aluminum at low temperatures. This is incorrect. The NPA method applies seamlessly from solid to liquid to plasma as long as there are 'free' electrons in the

system. We even predicted the crystalline $S(k)$ and calculated phonons along all standard directions in the Brillouin zone [16]. Furthermore, the first applications of the NPA methods were to solids at $T = 0$ published decades ago by Dagens [19] who calculated ground state energies and band structures for aluminum and other *simple metals*. Here and elsewhere we use the appellation ‘simple metal’ in a standard way, as used in Ashcroft and Mermin [17] and in other other standard works. For example, Rossiter (Ref. [18], p13) defines the term ‘simple metal’ to mean ‘virtually all electrons at the Fermi surface are *s*-like’.

The NPA results for solids are in good agreement with other available methods [19]. Our NPA model is not only a finite- T generalization of earlier models like those of Dagens, but also includes the property that the NPA is not just an approximation limited to non-overlapping muffin-tin average atoms. It is *an exact reduction* of the N -ion DFT problem to a single ion problem when a proper ion-ion correlation functional is used [20]. So we do not use the muffin-tin approximation for the continuum electrons, commonly invoked in average-atom(AA) models. Very little attention to this comprehensive DFT approach has been paid, some exceptions being the work of Chihara [21, 22], Ichimaru *et al* [48], Xu and Hansen [23].

Only the $S(k)$ near $2k_F$ is relevant to σ , and not k values outside the window of integration $f(k)\{1-f(k)\}$ in the Ziman formula. Since Sperling *et al.* used $S(k) = 1$, with not even a scalar- k dependence, we proposed a well-known approximation with about 20% error for single crystals and no error for powders. Such approximations, and the nearly-free electron Ziman formula are widely used [18].

Witte *et al.* have *not* presented a DFT-MD-KG calculation of the $2T$ -WDM conductivity to estimate (the non-spherical or) any contribution whatever from their $S(k)$. In fact, DFT-MD-KG cannot provide Kubo-Greenwood conductivity results for solids or cold ions for reasons explained in sec. II B. the lowest- T σ reported by Witte *et al.* is for equilibrium $T_i = T_e = 0.15$ eV.

B. Why the DFT-MD-KG conductivity calculation fails for cold ions

The lowest temperature where Witte *et al.* have reported a conductivity for aluminum using the DFT-MD-KG method is 0.15 eV with the ion and electron temperatures equal, viz., $T_i = T_e$. In $2T$ -ultrafast applications T_i is less than the melting point T_m and the DFT-MD-KG method becomes impractical for such cold ions as may be clear from the following discussion.

The DFT-MD-KG method attempts to represent the plasma ions by an ordered periodic crystal with a unit cell containing $N \sim 100 - 200$ atoms per ionic species for which a band structure is calculated for that particular crystal, although no such bands exist in a plasma. This highly unrealistic model has to capture the atomic and

electronic disorder found in the real sample by evolving it in time at the temperature T_i and generating many realizations of crystal configurations, with each yielding a dynamic conductivity for the resultant ionic configuration. Then a Drude model has to be applied to obtain a static conductivity, using the ‘mean-free path’ approximation for each case, as may be seen in a typical calculation like Ref. [10]. Then an average over all such individual ‘runs’ is made to obtain a static conductivity which is identified with that of the plasma. This process is an extremely computer-intensive and also time consuming process, and becomes impractical for cold ions which require many many time steps to generate new equilibrium ionic configurations. Alternatively, very large unit cells as recommended by Pozzo *et al.* [24] may be required to assure self averaging.

This serious bottleneck probably explains why Witte *et al.* have not provided UF-conductivities or equilibrium conductivities (with or without a spherical average) at the melting point T_m .

C. The excellent accord between our XRTs calculation and that of Witte *et al.* — Comment item (ii)

This comment has two parts. (a) After displaying the $S(\vec{k})$ of lattice-like aluminum in Fig. 1 of the Comment, Witte *et al.* state the following.

“Furthermore, DWD [2] claim, ‘The excellent accord between our XRTS calculation and that of Witte *et al.* (sic) are fully consistent with ... DFT-MD simulations.’ This statement is invalid ... In addition to the missing diffraction peaks ...”

Our claim of an excellent accord, given in DKHL Appendix, Sec.1 (lines 690-696, and 705-709) entitled: “1. X-ray Thomson scattering calculation for Li ...” is unambiguously *not* about aluminum crystals. No Laue peaks are expected for Li WDM at $T_i = T_e = 4.5$ eV. Fig. 9 of Ref. [3] displays the excellent agreement between the DFT-MD and NPA calculations, irrespective of the XC-functional used.

(b) WitteC lists the shortcomings of the Ziman formula, already discussed by Dharma-wardana *et al.* in e.g., Refs. [25–27]. Our objective in DKHL was to use

- the simplest NPA, XC-functional in the local-density approximation (LDA),
- weak local pseudopotentials,
- the nearly-free electron independent-scatterer Ziman formula.

to assess the quality of the so obtained WDM conductivities. We are well within experimental error or within 20% where accurate experimental data are available. large- N DFT-MD-KG, fancy XC-functionals etc., seem to do worse with σ_{ic} falling below experimental σ_{ib} (see below,

section VIII A) for low T . As for average atom (AA) models, they fail for low- T where test data are reliable.

WitteC ignores the short-comings of the DFT-MD-KG approach and provides evidence for the numerical convergence of their simulations with N up to 216 in their Fig. 4. As shown in sec. VIII A such converged results for the HSE or PBE functionals significantly violate known bounds, predicting $\sigma_{ic} < \sigma_{ib}$ at low T . This does not seem to be a problem linked to the XC-functional. MD-KG treats a plasma as an average over a sequence of crystals with band-structure. Only the dynamic conductivity $\sigma(\omega)$ is given by the KG formula. The latter uses various assumptions (e.g., single electron states, mean free-paths etc., that are also used in the Ziman formula), as well as the Drude model. Also, no valid derivation of the $T_i \neq T_e$ UFM KG formula exists, and the limit $\omega \rightarrow 0$ does not exist.

The DFT-MD-KG community uses the Kohn-Sham eigenstates of fictitious non-interacting Kohn-Sham electrons, instead of true electron eigenstates or approximate Dyson eigenstates [28], (see: DKHL, Sec. 2 of the Appendix, line 816). Local-field factors (LFFs) $G_{ei}(q)$ that moderate the electron-ion interaction $U_{ei}(q)$, being dominated by the small- q limit (c.f., compressibility sum rule) are poorly captured by small- N simulations, e.g., $N = 64$. Witte et al have given $N = 216$ simulations for some cases and argued that the $q \rightarrow 0$ issues cannot be a problem, but their calculations, while revealing the problem, do not resolve it. We take up this discussion further in sec. VIII A.

III. WITTE COMMENT ITEMS III AND IV

These items refer to DW16 and will not be treated here.

IV. STATIC CONDUCTIVITY OF ALUMINUM AND AVERAGE-ATOM (AA) MODELS — COMMENT ITEM (V)

WitteC's claim that NPA cannot capture the non-Drude behaviour of $\sigma(\omega)$ near $\omega \sim E_F$ is incorrect. The NPA phase shifts are used to calculate the modified density of states (DOS), impose the Friedel sumrule, and calculate a \bar{Z} consistent with the modified DOS (see Eq. A2, Appendix to DKHL). The non-Drude features arise from the modified DOS. Such NPA calculations for the DOS agree with DFT calculations, even for complex fluids like carbon and Si, as shown by Dharma-wardana and Perrot in 1990 [29]. An effective mass m^* accounts for the modified DOS in 'simple' metallic C, Si systems [30]. A detailed response regarding this is more appropriately relegated to a proposed reply to the comments by Witte *et al* on DW16.

Figure 3(a) of the Witte comment shows DFT σ_{ic} for Al at $T_i = T_e$ taken to high temperatures $T > E_F$ (see

Fig. 4). But serious questions arise.

(i) WitteC compares equilibrium data with the *non-equilibrium* Milschberg data for σ_{uf} . This pioneering experiment [31] is irrelevant to $T_i = T_e$ systems. Furthermore, Ref. [31] used an over-simplified data reduction, and better models give a different T -dependence [32, 33]. Nevertheless, intuitive plasma models have been constructed to give conductivity results that mimic the results of the Milschberg data. Some of these AA models which use the thermodynamic potential of mean force rather than the electron-ion potential will be reviewed below, in sec. V.

(ii) As laser excitations couple with the free electrons, three electrons per ion ($\bar{Z}=3$) are heated in Milschberg-type experiments using initially solid Al. The $T_i \neq T_e$ Ziman calculations reproduce the minimum seen in the conductivity. Dharma-wardana and Perrot demonstrated such a minimum in 1992 in Ref. 34 when the ionization \bar{Z} is held fixed. However, \bar{Z} increases with increasing T . Ionic mixtures with $\bar{Z} = 3 \rightarrow 4 \rightarrow 5 \rightarrow 6$ occur for T in the 8-50 eV range. DFT-MD beyond 8 eV, to 15 eV (as in the Witte comment) encounters $Z = 3, 4$ ionized Al. Such DFT-MD simulations need at least some 100 atoms *per species* in DFT-MD simulations to obtain $S(q), G_{ei}(q)$, and transport properties. Witte *et al.* have used only 64 atoms. This is totally inadequate for ionic mixtures containing several types of ions with different ionizations. To clarify matters, we study such a mixture of ionic species [35].

V. RESULTS FOR A MIXTURE OF IONIC SPECIES.

In the NPA model, the free-electron pileup $\Delta n(r)$ around an aluminum nucleus immersed in the appropriate plasma medium is used to construct a weak *local* pseudopotential whose Fourier transform, $U(q)$ is given by

$$U(q) = \Delta n(q)/\chi(q) \quad (1)$$

This scheme is appropriate for 'simple metals' but not transition metals where the electrons at the Fermi surface are not *s*-like. Here $\chi(k)$ is the interacting density-density linear-response function at finite temperature and at the given electron density. This response function includes finite- T local field factors constructed to satisfy the compressibility sumrule, as discussed in previous publications [3, 35]. The resulting pseudopotentials are fitted to the parametric form given in Eq. 60 of Dharma-wardana and Perrot [36] where the Heine-Abarankov form is generalized via the modulating function $M(q)$. This better accounts for the $q > 2k_F$ regime by having two extra parameters λ and q_0 . The *e-i* interaction $U_{ei}(q)$ is written here with the subscripts *ei* suppressed for brevity.

$$U(q) = U_{HA}(q)M(q), \quad (2)$$

$$M(q) = \{1 + \lambda(q/q_0)^2\}/\{1 + (q/q_0)^2\}. \quad (3)$$

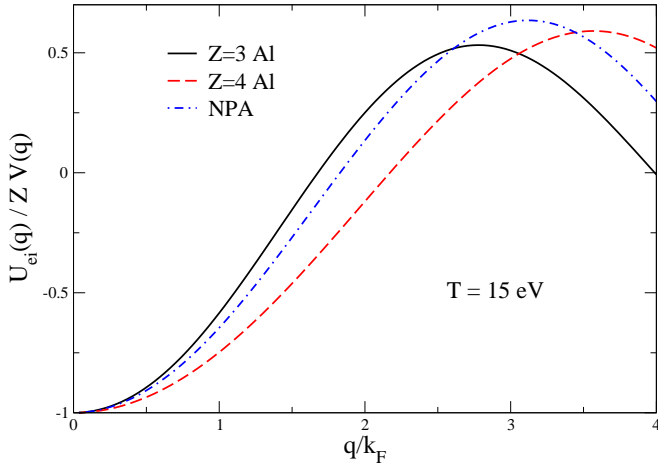


FIG. 3. (Color online) The pseudopotentials for the ionization species $s=1,2$, with integer ionizations $Z_s=3$ and 4 are compared with the NPA pseudopotential with a mean ionization $\bar{Z} = 3.17$ applicable at $T = 15$ eV. The quantity plotted is the pseudopotential $U_{es}(q)/ZV_q$, i.e., in units of the bare electron-ion interaction $ZV_q = 4\pi Z/q^2$ (atomic units). The plasma density is 2.7 g/cm^3 with a mean ion-ion $\Gamma \simeq 6.1$.

TABLE I. The composition fractions $x_s, s = 1, 2, 3$ for the ionic species Al^{z+} , with integer ionizations $Z_s = 3, 4, 5$ in the temperature range 10-40 eV for an aluminum plasma at the density $\rho = 2.7 \text{ g/cm}^3$.

T [eV]	$x_1, Z = 3$	$x_2, Z = 4$	$x_3, Z = 5$
10	0.970	0.030	0.00
15	0.830	0.170	0.00
25	0.110	0.890	0.00
35	0.0	0.300	0.70
38.8	0.0	0.001	0.99

The pseudopotentials for the individual species are used to construct the pair-potentials $V_{ss'}(q)$, given by:

$$V_{ss'}(q) = Z^2 V_q + U(q)_{es}(q) \chi(q) U_{es'}(q). \quad (4)$$

They are used in a multi-species hyper-netted-chain (HNC) calculation yielding the pair-distribution functions (PDFs) $g_{ss'}(r)$, and structure factors $S_{ss'}(q)$. These can be used to construct the equation of state (EOS) of the multi-species plasma in the HNC approximation as detailed in Ref. [35]. For temperatures below 1 eV, a bridge-diagram correction is included in the HNC, using the hard-sphere ansatz as detailed in Ref. [37]. That is, we use the modified HNC equation with a bridge contribution that assures that the compressibility obtained from the EOS is in agreement with the $S_{ii}(q \rightarrow 0)$ limit. The simple HNC equation is sufficient for $T > 1$ eV. Although the appendix to Ref. [35] presented the details of the core-core polarization contributions to the pair potential, we neglect them in this study. Since our focus here is the conductivity, we do not discuss the EOS results, but consider the Ziman formula for a mixture of

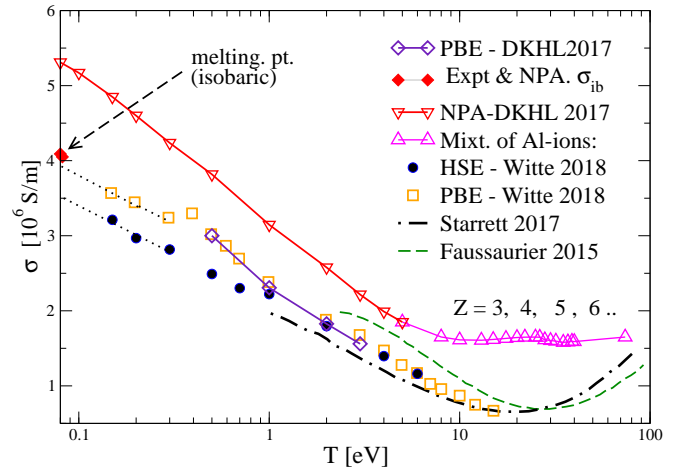


FIG. 4. (Color online) The σ_{ic} from two recent AA models display a broad minimum for 20-30 eV. The 64-atom simulations of Witte *et al.* show the same trend. For $T > 5$ eV the conductivity of the multispecies NPA plasma [35] shows a weak rise in σ_{ic} at 26.34 eV when $Z = 4$ holds. The MD-DFT-KG σ_{ic} , $T \rightarrow 0.082$ eV incorrectly extrapolate to below the red diamond, i.e., the *isobaric* melting-point conductivity. See Eqn. 9 for the consistency of $\sigma_{ic} \simeq 5 \times 10^6 \text{ S/m}$ obtained from the NPA at 0.082 eV with the experimental isobaric value. See Sec. VI of SM for details.

ions giving the resistivity $R = 1/\sigma$.

$$R = \frac{\hbar}{e^2} \frac{1}{3\pi} \frac{\rho}{\bar{n}^2} \quad (5)$$

$$\times \int_0^\infty (1 + \exp\{\beta q^2/8 - \mu\})^{-1} q^3 \Sigma(q) dq, \quad (6)$$

$$\Sigma(q) = \sum_{s,s'} (x_s x_{s'})^{1/2} S_{ss'}(q) \frac{U_{es}(q) U_{es'}(q)}{\{2\pi\epsilon(q)\}^2} \quad (7)$$

The resulting conductivity for an ionic mixture is displayed in Fig. 4. together with other calculations. It shows that DFT-MD-KG calculations give a significantly lower isochoric conductivity than from the NPA-mixture calculation, and extrapolates to a value below the isobaric conductivity at the melting point. One possible problem is the limitation of the DFT-MD-KG calculations to 64 atoms; In a 64-atom simulation with even two species, i.e., 32 atoms/per species, the ‘surface’ atoms of the simulation cluster dominate over the ‘bulk-like’ atoms. The LFF $G_{ei}(q)$ is known to be mostly set by the value of $G_{ei}(q \rightarrow 0)$ due to the importance of the compressibility sum rule. But this is poorly captured by small- N simulations in much the same way as how they poorly reproduce the small- q behaviour of $S(q)$. From Fig. 4 of WitteC we see that a 32 atom calculation may significantly underestimate a larger- N calculation. In effect, if there are m ionic species in the system, the simulation must use $\sim 100m$ particles to have the quality of a 100-atom single species simulation. (see also Sec. VIII).

It should however be noted that the calculations of Witte in the low temperature range (where $Z = \bar{Z} = 3$) cannot be faulted for the use of a small N since they have shown results for $N = 214$. Hence the under-estimate of the low-temperature σ_{is} (and indeed even σ_{ib}) become an intriguing problem. Perhaps very large N simulations are needed, as posited by Pozzo *et al* for the case of the low-temperature conductivity of WDM sodium.

VI. THE ROLE OF ELECTRON-ELECTRON AND ION-ION INTERACTIONS IN ELECTRON SCATTERING IN THE 5 EV TO 50 EV REGIME.

We examine Starrett’s approach [38] to define what he explains to be the “interaction potential between the scattering electron and the ion so that it correctly includes the effects of ionic structure, screening by electrons and partial ionization”. As already stated, various attempts to use the potential of mean force and the XC-potential as scattering potentials need a rigorous derivation based on the current-current correlation function or some such basic transport theory.

The Ziman formula is based on the force-force correlation function. The Ziman formula that we use for these calculations, viz., Eq. 5 uses a single scattering center and the effect of the other scatters is brought in via the ion-ion partial structure factors $S_{ss'}(k)$ which are related by a Fourier transform to the pair correlation functions $h_{ss'}(r) = g_{ss'}(r) - 1$. The single scatterer model fails in many circumstances and a multiple scattering model is then needed. A measure of the strong coupling present in a plasma is given by the parameter $\Gamma = Z^2/(r_{ws}T)$. For our system, (T, Γ) is such that we have (10,8.4); (20,5.5); (30,5.6); (40,5.9); (60,5.9); (80,6.0). These numbers show the phenomenon of the approximately constant ‘ Γ -plateau’ that has been discussed by Cl  rouin *et al.* [39]. The Al-plasma in the regime where the AA models find a broad conductivity minimum has a $\Gamma \sim 5 - 6$. The Al-Al average-atom ion-ion structure factor $S_{ii}(q)$ for the cases $T = 5, 15, 25, 35$ eV are shown in Fig. 5. Hence we believe that multiple-scattering effects are irrelevant in this regime, and the Ziman formula, i.e., Eq. 5 holds.

Furthermore, we look at the ion-ion and electron-electron pair-distribution functions (PDFs) relevant to the aluminum plasma of density 2.7 g/cm^3 in the temperature range 5-50 eV. If phase-shifted plane-wave states are an adequate representation of the wave functions of the continuum electrons, then electron-electron scattering does not contribute to the resistivity as the electron momentum is a ‘good quantum number’ [40]. In contrast, the Boltzmann equation uses no concepts of eigenstates, and *assumes* momentum randomization after each collision and always contains e-e contributions to electron scattering. In any case, e-e scattering calculated within such models makes only a minor contribution to the resistivity in high- Z materials like aluminum. Hence it is unlikely that Starrett’s calculations would contain signif-

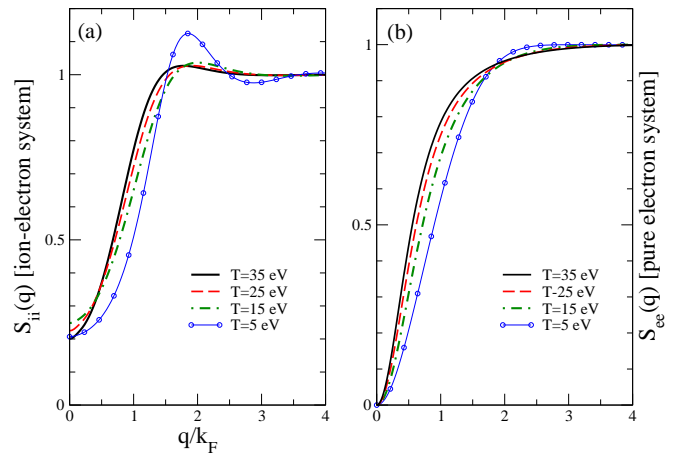


FIG. 5. (Color online)(a) The ion-ion structure factor $S_{ii}(q)$ from the NPA potentials, for aluminum plasmas (2.7 g/cm^3) with $T = 5$ eV to 35 eV. (b) The electron-electron $S(q)$ for a *pure* electron fluid at the densities and temperatures corresponding to those of the aluminum plasma is given mainly to illustrate the weak coupling nature of the fluid.

TABLE II. The average bound-state radii $\langle r_{nl} \rangle$ (in a.u.) of the NPA model for the $2s$ and $2p$ atomic states of the aluminum plasma in the temperature range 10–35 eV, density $\rho = 2.7 \text{ g/cm}^3$, $r_{ws} \simeq 3$ a.u.

T [eV]	$\langle r_{2s} \rangle$	$\langle r_{2p} \rangle$
10	0.984	0.016
15	0.830	0.170
25	0.110	0.890
35	0.5814	0.5384

icant e-e scattering contributions to the conductivity.

Electron-electron scattering can be relevant in systems where the particulate nature of the electron subsystem becomes relevant. If the electron distribution is ‘grainy’ or ‘disordered’ within the relevant length scale, then the system is in the ‘diffusive regime’ where planewave states are no-longer good eigenstates of the Hamiltonian. In such systems the electron-electron structure factor and the pair-distribution function will show the characteristics of a disorder-dominated fluid, in the diffusive regime. Then indeed e-e interactions may contribute to the electrical resistivity. This is surely not the case here.

The XC-potential acts on (fictitious) Kohn-Sham electrons which are non-interacting but at the density of the interacting system to provide a many-body correction to the free energy. It does not act on “real” electrons as applicable in conductivity equations.

The ion-ion structure factor $S_{ii}(q)$ and the electron-electron structure factor $S_{ee}(q)$ are of interest in understanding the interplay of many-body interactions. The $S_{ii}(q)$ obtained from the NPA model is readily available and shown in Fig. 5(a). The agreement of the NPA calculated $S(q), g(r)$ with those from X-ray scattering experiments on liquid metals, and with DFT-MD has been

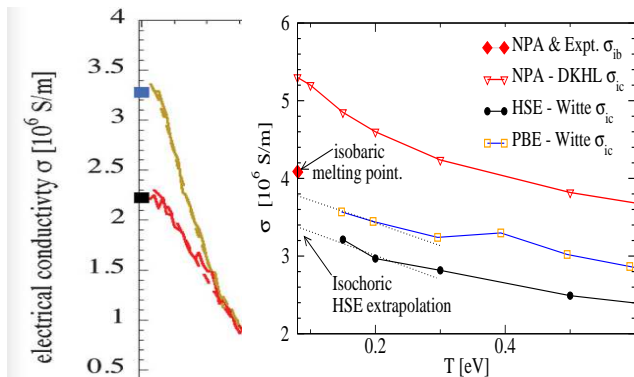


FIG. 6. (Color online) **Left Panel:** Extract from Fig. 1 of Witte *et al.* [4] displaying converged $\sigma_{ic}(\omega)$ plots for isochoric Al at 0.3 eV for small ω . The upper curve extrapolating towards 3.5 is using the PBE, while the lower curve (extrapolating towards ~ 2.4) is obtained using the HSE functional. **Right Panel:** The behaviour of σ_{ic} as $T \rightarrow T_m$ from different calculations. These presumably “well-converged” DFT-MD-KG results extrapolate to a value even *below* the known experimental isobaric conductivity of aluminum at its melting point $T_m = 0.082$ eV [42].

established in many publications, the most recent being in Ref. [46] in regard to aluminum.

An approximation to $S(q)$ can be readily calculated in the Γ -plateau region using the classical one-component plasma (OCP) model containing only ions neutralized by a uniform static background. Such an approximation will get the ‘main peak’ region right, but it will be seriously wrong mainly in the small- q region, unlike the result obtained via the NPA where the compressibility sumrule is satisfied. The $S_{ee}(q)$ shown in Fig. 5(b) is for a fully interacting pure electron plasma (a quantum OCP) where quantum effects are included via the classical-map hypernetted-chain (CHNC) procedure [41]. We do not attempt to calculate the $S_{ee}(q)$ in the presence of the ions as such a calculation satisfying the sumrules as well as the quantum mechanics of the coupled electron-ion system is a more complex task not required for this study, requiring the use of a three component CHNC model for aluminum.

However, the main change will be the modification of the small- q region of $S_{ee}(q)$ to conform with those of $S_{ii}(q)$ so as to satisfy the compressibility sum rule for an electron-ion system. However, the essential point to note is the clearly weakly-coupled nature of the interactions present in these systems, as well as the fact that the electron-ion interaction (Fig. 3) can be given as a weak local pseudopotential. Hence, in our view, the attempt to invoke e-e scattering and contributions to the scattering potential from ion-ion interactions, other than those which enter in the standard theory via the LFF $G_{ei}(q)$ of e-i interaction, and the LFFs that enter into the dielectric function, remains unsubstantiated even within an intuitive physical picture.

VII. KOHN-SHAM LEVEL STRUCTURE OF THE ALUMINUM PLASMA

Average atom calculations as well as NPA calculations require special procedures if bound-states stretch out beyond the Wigner-Seitz sphere of the ion, as is typically the case for transition-metal ions. The Wigner-Seitz radius $r_{ws} \simeq 3$ a.u. for aluminum at 2.7 g/cm³. In Table II we present the radial extension of the $n = 2$ bound states of the NPA for typical cases in the temperature range $T=10$ to 35 eV. The NPA bound states are compactly within the Wigner-Seitz sphere and no difficulty arises from bound-like continuum resonances, and ‘discontinuous’ changes in \bar{Z} in the NPA. The bound levels are compact in the respective ionization states ($Z=3,4, 5$ models) needed for the multi-species plasma.

VIII. CONVERGENCE OF DFT-MD-KG CALCULATIONS

In WitteC it is stated that “DWD finds larger dc conductivities from NPA-Ziman calculations compared to DFT and attributes this partly to the ‘inability of the DFT-MD-KG approach to access small- k scattering contributions unless the number of atoms N in the simulation is sufficiently large.’ The criticism on Refs. [4, 36], however, is not valid. Note that several earlier studies reported well-converged conductivity calculations for aluminum and lithium with similar particle numbers [35, 37-39]”.

The issue is not just numerical convergence as a function of N as seen by the increasing closeness of the $\sigma(\omega)$ curves, but also the question of whether the results approach the expected experimental values, or converge to a different bound. In the right panel of Fig. 6 we show results from two presumably well-converged calculations for σ_{ic} of aluminum (2.7 g/cm³) given by Witte *et al.*, one of which uses the first-principles PBE XC-functional, while the lower estimate of σ_{ic} uses the semi-empirical HSE functional which incorporates an *ad hoc* Hartree-Fock contribution adjusted to get bandgaps correct.

We have tentatively indicated an extrapolation towards the melting regime (0.082 eV for isobaric Al) using thin dotted lines, for these two sets of calculations. These show that *both* KG calculations predict a σ_{ic} at 0.082 eV that are *even lower* than the experimentally known isobaric conductivity of 4.1×10^6 S/m. In fact, the most recent ‘well-converged’ HSE prediction [10] extrapolates towards 3.5×10^6 S/m. The isochoric conductivity of aluminum, density 2.7 g/cm³ *cannot* be any smaller than the isobaric conductivity at the lower density of 2.375 g/cm³, but the KG simulations strongly contravene this.

The scaling of the known experimental isobaric conductivity to the isochoric conductivity can be discussed as follows, where we correct an expression given by Witte *et al.* in their comment.

Witte *et al.* relate σ_{ib} to σ_{ic} incorrectly using only the

volume change. They ignore the change in the scattering cross-section Σ due to the changed screening. But in bringing out this discussion, Witte *et al* seem to recognize the *physical requirement* resulting from the consequent physics. That is:

$$\sigma_{ic} > \sigma_{ib} \text{ for Al.} \quad (8)$$

At low $T \ll E_F$, scattering occurs with a momentum transfer of $\sim 2k_F$ where $\Sigma \sim |V(2k_F, \rho)|^2$, with $\Sigma \propto \{\bar{Z}/(|4k_F^2 + k_{sc}^2|)\}^2$. Here k_{sc} is the T, ρ dependent Thomas-Fermi screening wavevector. Thus,

$$\sigma_{ic} = \sigma_{ib} \frac{\rho_{ic}}{\rho_{ib}} |X_{ic}/X_{ib}|^2 \quad (9)$$

$$X_{ib} = |4k_F^2 + k_{sc}^2|_{\text{at } \rho_{ib}}; \text{ similarly, for } X_{ic}. \quad (10)$$

This provides a consistency test (at very small T/E_F) relating the experimental σ_{ib} and σ_{ic} .

This equation shows that σ_{ic} should be $\sim 5 \times 10^6$ S/m at the melting point. While the NPA correctly captures this value, the KG simulations fall far short. In fact, the the HSE functional which is strongly promoted in Witte *et al.* [4] gives a σ_{ic} that is a gross underestimate of the true σ_{ic} by 150%. In DKHL we merely gave some suggestions as to why such a discrepancy should arise. These were (i) theoretical short-comings of the KG formula (ii) possible limitations in the N -simulation to accurately capture the LFFs that are implicit in the effective electron-ion scattering which are dominated by the $q \rightarrow 0$ limit. However, given the extensive simulations of Witte *et al.*, item (ii) may not be relevant. However, the N -convergence studies up to $N=216$ presented in WitteC provide no solution to the puzzle.

All DFT XC functionals should recover the STATIC properties of simple or complicated material systems, but they *need not* recover band gaps and spectra as DFT is NOT a theory of such properties. So, if HSE gives better bandgaps and features of the excitation spectrum, Cooper minima etc., due to the inclusion of *ad hoc* corrections into it, those seeming improvements cannot be at the sacrifice of *static* properties. If static properties related to the total free energy or the ground state are sacrificed by a proposed XC functional, then it has fallen outside DFT variational principles.

It is clear that having seemingly N -converged KG simulations do not guarantee an accurate prediction of the conductivity. Thus fig. 4(c), (d) of WitteC merely establish that their best converged results actually strongly violate the physical condition given in Eq. 1. In regard to Fig. 4 (d) of WitteC, what one would like to know is the estimate of the compressibility from the $S(q \rightarrow 0)$ limit at each N and the extent of its disagreement with the compressibility obtained from the corresponding equation of state, for PBE and HSE.

Interestingly, the offset between the expected value of σ_{ic} at $T_m = 0.82$ eV, viz., 5.1×10^6 S/m and the PBE or HSE- $\sigma_{ic} = 3.4 \times 10^6$ S/m is nearly the same as the offset of the broad minima of the NPA mixture calculation with those from DFT-MD-KG and AA calculations in the 25 eV range.

A. Gathers's corrections of raw experimental data - Witte comment vi

We are satisfied that Witte *at al.* now recognize that Gathers' data are isobaric. Gathers' column 4, column 5 data differ only by *about* 0 – 25%, and the difference arising from XC-functionals is similar. Hence our main concerns are resolved, irrespective of the data column used. Nevertheless, we examine WitteC, item (vi) further.

Gathers *explicitly states* that the data are applicable only in the density range $2.42 \geq \rho \geq 1.77$ g/cm³ in both Ref. 14 and in Ref. 7. He states that the enthalpy H needs a dilation correction v/v_0 and this not a crude correction to get σ_{ic} at 2.7 g/cm³. And yet, even though extrapolation of the conductivity data to 2.7 g/cm³ is explicitly forbidden, Witte *et al.* say “*We agree that this extrapolation to σ_{ic} made by Gathers is crude ...*”.

Gathers' 1986 review [14] was after Desai's work [45]. The converged HSE σ of WitteC falls below Gathers' data [7, 14] by $\sim 20\%$.

B. Comment on the XC-functional — item (viii) of Comment

The *static* conductivity is an equilibrium ensemble property and should be captured by standard DFT. Given that Witte *et al.* have revised their value of σ_{ic} from the HSE functional, and since even AA models can pick up the non-Drude behaviour of $\sigma(\omega)$ as stated by WitteC, there is finally no compelling evidence in favour of the HSE functional which has an *ad hoc* inclusion of a quarter of a Hartree-Fock term.

IX. CONCLUSION

The Witte-comment and also Ref. [10] show a welcome revision where they no longer claim that the static conductivity of aluminum at $T = 0.3$ eV and density 2.7 g/cm³ varies by large factors like ~ 1.5 on changing the XC-functional from PBE to HSE. The *ad hoc* HSC functional gives less satisfactory static σ predictions. Equilibrium isochoric aluminum conductivity at higher T [10] where there are several ionization states will require simulations with some 200-300 atoms for credible results.

[1] B. B. L. Witte et al., Phys. Rev. E, **99**, 047201 (2019)

[2] M. W. C. Dharma-wardana, Phys. Rev. E **93**, 063205 (2016).

- [3] M.W.C. Dharma-wardana, D. D. Klug, L. Harbour, Laurent J. Lewis, Phys. Rev. E **96**, 053206 (2017).
- [4] B. B. L. Witte, L. B. Fletcher, E. Galtier, E. Gamboa, H. J. Lee, U. Zastra, R. Redmer, S. H. Glenzer, and P. Sperling Phys. Rev. Lett. **118**, 225001 (2017).
- [5] J. Heyd, G. E. Scuseria, and M. Ernzerhof, J. Chem. Phys. **118**, 219906 (2003).
- [6] J. P. Perdew, K. Burke and M. Ernzerhof, Phys. Rev. Lett. **77**, 3865 (1996).
- [7] G. R. Gathers, Int. J. Thermophys. **4**, 209 (1983).
- [8] V. Vlček, N. de Koker, and G. Steinle-Neumann, Phys.Rev. B **85**, 184201 (2012).
- [9] T. Sjoström, and Jérôme Daligault, Phys. Rev E **92**, 063304 (2015).
- [10] B. B. L. Witte, P. Sperling, M. French, V. Recoules, S. H. Glenzer, and R. Redmer, Physics of Plasmas **25**, 056901 (2018).
- [11] V E Fortov, V V Yakushev, K L Kagan, I V Lomonosov, E G Maksimov, M V Magnitskaya, V I Postnov and T I Yakusheva J. Phys. Condens. Matter **14**, 10809 (2002).
- [12] M. Bastea and S. Bastea, Phys. Rev. B **65**, 193104 (2002).
- [13] Witte, B. B. L., and Shihab, M. and Glenzer, S. H. and Redmer, R. Phys. Rev. B, **95**, 144105 (2017).
- [14] G. K. Gathers, Reports on Progress in Physics, **49** no:4, 341 (1986).
- [15] P. Sperling, E. J. Gamboa, H. J. Lee, H. K. Chung, E. Galtier, Y. Omarbakiyeva, H. Reinholz, G. Röpke, U. Zastra, J. Hastings, L. B. Fletcher, S. H. Glenzer, Phys. Rev. Lett. **115**, 115001 (2015).
- [16] L. Harbour, M. W. C. Dharma-wardana, D. D. Klug, L. J. Lewis, Phys. Rev. E **95**, 043201 (2017).
- [17] N. W. Ashcroft and N. D. Mermin, *Solid State Physics*, Saunders College, Philadelphia, USA (1976)
- [18] P. L. Rossiter, The electrical resistivity of metals and alloys, Cambridge University Press (1987).
- [19] L. Dagens, J. Phys. (Paris) **36**, 521 (1975).
- [20] M. W. C. Dharma-wardana and F. Perrot, Phys. Rev. A **26**, 2096 (1982).
- [21] J. Chihara, J. Phys. C **19**, 1665 (1986).
- [22] J. Chihara, High Energy Density Physics **19** 38, (2016).
- [23] Hong Xu and J. P. Hansen, Physics of Plasmas **9**, 21 (2002)
- [24] Monica Pozzo, Michael P. Desjarlais, and Dario Alfè, Phys. Rev. B, **84**, 054203 (2011).
- [25] F. Perrot, M.W.C. Dharma-wardana, Phys. Rev. A **36** 238–246 (1987).
- [26] F. Perrot *et al.* Int. J. of Thermophys, **20**, 1299 (1999).
- [27] M.W.C. Dharma-wardana in *Laser Interactions with Atoms, Solids, and Plasmas*, Cargèse NATO workshop, 1992, Edited by R.M. More (Plenum, New York, 1994), p 311.
- [28] F. Perrot and M. W. C. Dharma-wardana, Phys. Rev. A **29**, 1378 (1984).
- [29] M. W. C. Dharma-wardana and F. Perrot, Phys. Rev. Lett., **65**, 76 (1990).
- [30] M. W. C. Dharma-wardana, Phys. Rev. E **86**, 036407 (2012).
- [31] H. M. Milchberg, R. R. Freeman, S. C. Davey, and R. M. More, Phys. Rev. Lett. **61**, 2364 (1988).
- [32] A. Forsman, A. Ng, G. Chiu and R. M. More, Phys. Rev. E **58**, R1248 (1998).
- [33] A. Ng, T. Ao, F. Perrot, M.W.C. Dharma-wardana, M.E. Ford, Laser and particle beams, **23**, 527-537 (2005). <https://doi.org/10.1017/S0263034605050718>
- [34] M.W.C. Dharma-wardana and F. Perrot, Phys. Lett. A **163**, 223 (1992).
- [35] F. Perrot, and M.W.C. Dharma-wardana, Phys. Rev. E. **52**, 5352 (1995).
- [36] M. W. C. Dharma-wardana, and François Perrot, Phys. Rev. E **58**, 3705 (1998)
- [37] F. Perrot, Phys. Rev. E **47**, 570 (1993).
- [38] C. Starrett, High Energy Density Physics **25**, 8 (2017).
- [39] J. Clérouin, Ph. Arnault, G. Robert C. Tیکنور, J. D. Kress, L. A. Collins Contributions to Plasma Physics (Beiträge aus der Plasmaphysik) 55(2-3) (2014) <https://onlinelibrary.wiley.com/doi/pdf/10.1002/ctpp.201400064>
- [40] M. W. C. Dharma-wardana, Phys. Rev. E **73**, 036401 (2006)
- [41] M. W. C. Dharma-wardana and F. Perrot, Phys. Rev. Lett. **84**, 959 (2000)
- [42] The experimental value and theoretical estimates are quoted in R. Leavens, A. H. MacDonald, R. Taylor, A. Ferraz, and N. H. March, Phys. Chem. Liq. **11**, 115 (1981).
- [43] F. Perrot, Y. Furutani and M.W.C. Dharma-wardana, Phys. Rev. A **41**, 1096-1104 (1990)
- [44] J. A. Porter, N. W. Ashcroft and G. V. Chester, Phys. Rev. B **81**, 224113 (2010).
- [45] P. D. Desai, H. M. James, and C. Y. Ho, J. Phys. Chem. Ref. Data **13**, 1131 (1984).
- [46] Harbour, L. and Förster, G. D. and Dharma-wardana, M. W. C. and Lewis, Laurent J. Physical review E **97**, 043210 (2018).
- [47] Hannes R. Rüter and Ronald Redmer, Phys. Rev. Lett. **112**, 145007 (2014).
- [48] X.-Z. Yan, S. T. Tsai, and S. Ichimaru, Phys. Rev. A **43**, 3057 (1991).